Mathematical Medicine and Biology: A Journal of the IMA (2019) **00**, 1–14
doi:10.1093/imammb/dqz002

Analytic solutions for calcium ion fertilisation waves on the surface of eggs

Bronwyn H. Bradshaw-Hajek*
School of Information Technology and Mathematical Sciences, University of South Australia, Mawson Lakes, SA 5095, Australia
*Corresponding author. Email: bronwyn.hajek@unisa.edu.au

and

Philip Broadbridge
Department of Mathematics and Statistics, La Trobe University, Victoria 3086, Australia

[Received on 12 September 2018; revised on 12 December 2018; accepted on 12 December 2019]

The evolution of calcium fertilisation waves on the cortex of amphibian eggs can be described by a nonlinear reaction-diffusion process on the surface of a sphere. Here, we use the nonclassical symmetry technique to find an exact analytic solution that describes the evolution of the calcium concentration. The solutions presented compare well with published experimental results. The analytic solution can be used to give insight into the processes governing the fertilisation wave, such as the flow of calcium ions from the sperm entry point. By finding a spiral solution to an approximate equation linearised near saturation, we also demonstrate how solutions with other properties may be constructed using this technique.

Keywords: fertilisation waves; calcium waves; analytic solutions; Lie symmetry analysis;

1. Introduction

Calcium ion fertilisation waves travelling over the surface of fish eggs were first observed in the 1970's by Gilkey *et al.* (Gilkey, 1983; Ridgway *et al.*, 1977) and were subsequently observed in sea urchin, frog and mouse eggs, among others (Cuthbertson *et al.*, 1981; Steinhardt *et al.*, 1977; Wasserman *et al.*, 1980). Calcium ions diffuse from the sperm puncture point and stimulate further release from stores just beneath the surface. This increase in the cortical calcium ion concentration is necessary to block polyspermy and it also initiates key processes in the activation of the embryonic cell cycle (Nuccitelli, 1991; Wagner *et al.*, 1998).

A number of mathematical models describing the evolution of calcium waves in general, and calcium fertilisation waves in particular have been developed. Almost all of these models are of reaction-diffusion type and fall into one of two categories, as described by Tsai & Sneyd (2007). Some models consist of systems of differential equations and contain details regarding the various mechanochemical processes and descriptions of calcium pumps and channels, whereby stored calcium is released to the ovum surface (Sneyd *et al.*, 1993; Wagner *et al.*, 1998). Others consider only the essential mechanisms, ensuring that the model reflects the most important features while remaining mathematically tractable (Cheer *et al.*, 1987; Lane *et al.*, 1987; Tsai & Sneyd, 2007).

In this paper, we consider this second type of model and use nonclassical symmetry analysis look for exact analytic solutions of a nonlinear reaction-nonlinear diffusion equation

$$u_t = \nabla.(D(u)\nabla u) + R(u), \tag{1.1}$$

on the surface of a spherical egg, where ∇ is the usual gradient operator on the surface of a sphere. The diffusion coefficient, $D(u)$, is typically taken to be constant. Here, we use a cubic nonlinear reaction term (discussed in more detail in Section 2).

The classical Lie point symmetry classification of reaction-diffusion equations, with consequent similarity reductions, was presented by Galaktionov *et al.* (1988). The complete nonclassical symmetry classification for the case when $u(\mathbf{x}, t) = u(x, t)$ (i.e. one (Cartesian) dimension), and $D(u) = D$ is a constant, was given by Arrigo *et al.* (1994) and Clarkson & Mansfield (1994). Other solutions, particularly in the context of population dynamics and nerve impulses, are given in Kametaka (1976), McKean (1970), Conte (1988), Chen & Guo (1992), Chen & Gu (1999), Kawahara & Tanaka (1983) and Nikitin & Barannyk (2004). Solutions to the nonlinear diffusion equation in spherical coordinates, with $R(u) = 0$ and spherical symmetry were provided by King (1990). Nonclassical invariant solutions for nonlinear diffusion-nonlinear reaction in Cartesian coordinates were found by Arrigo & Hill (1995) and Goard & Broadbridge (1996).

In Section 2 we present the model in more detail and nondimensionalise the relevant equation. In Section 3, we describe the results presented in Arrigo & Hill (1995) and Goard & Broadbridge (1996) and extend them to the case of spherical coordinates. A specific example solution to the nonlinear model describing the evolution of the calcium fertilisation wave is presented in Section 4. In Section 5, we present some spiral solutions using an approximate linearised model that is valid near an equilibrium point. In Section 6 we make some final remarks and comment on the applicability of the solutions presented herein.

2. Model equations and nondimensionalisation

As described above, a number of reaction-diffusion models have been proposed to describe a calcium fertilisation wave on the surface of an egg. Here, we use a cubic reaction term so that our model equation in dimensional variables is

$$\bar{u}_{\bar{t}} = \bar{\nabla}.(\bar{D}(\bar{u})\bar{\nabla}\bar{u}) + \bar{s}(\bar{u} - \bar{u}_{\min})(\bar{u}_{\max} - \bar{u})(\bar{u} - \bar{u}_1), \tag{2.1}$$

where $\bar{u}(\bar{\theta}, \bar{\phi}, \bar{t})$ is the areal concentration of calcium ions, $\bar{u}_{\max}$ and $\bar{u}_{\min}$ are the maximum and minimum concentrations, respectively, $\bar{D}(\bar{u})$ is the nonlinear diffusion coefficient, $\bar{s}$ is a constant and $\bar{\nabla}$ is the usual (dimensional) gradient operator on the surface of a sphere. While this form of the reaction term captures some of the reaction kinetics (Cheer *et al.*, 1987; Lane *et al.*, 1987; Slepchenko *et al.*, 2000) and reflects the bistable nature of the problem (Cheer *et al.*, 1987; Tsai & Sneyd, 2007; Wagner *et al.*, 1998), the model is still mathematically tractable. Other relatively simple forms of the reaction term that may be considered include those derived from a Michaelis–Menton approach (Fall *et al.*, 2004).

Equation (2.1) with $D(u) = D$ (constant) has been used to model one-dimensional (planar) calcium waves (Sneyd *et al.*, 1998; Tsai & Sneyd, 2007), as well as calcium fertilisation waves on the surface of a sphere (Cheer *et al.*, 1987; Murray, 2002). The equation is often solved numerically, although Lane *et al.* (1987) constructs a solution to an approximate equation with piecewise linear $R(u)$.

Introducing the nondimensional (unbarred) variables $\bar{r} = ar$, $\bar{t} = Tt = (a^2/\langle\bar{D}\rangle)t$, $\bar{u} = Uu = (\bar{u}_{\max} - \bar{u}_{\min})u$ and $\bar{D}(\bar{u}) = \langle\bar{D}\rangle D(u)$, where

$$\langle\bar{D}\rangle = \frac{1}{U}\int_{\bar{u}_{\max}}^{\bar{u}} \bar{D}(\bar{u}')\mathrm{d}\bar{u}',$$

we rewrite (2.1) to obtain

$$u_t = \nabla.(D(u)\nabla u) + su(1-u)(u-u_1), \tag{2.2}$$

where

$$u_1 = \frac{\bar{u}_1 - \bar{u}_{\min}}{\bar{u}_{\max} - \bar{u}_{\min}} \quad \text{and} \quad s = T(\bar{u}_{\max} - \bar{u}_{\min})^2\bar{s}$$

($0 < u_1 < 1$) are positive nondimensional parameters. In this paper, we seek exact analytic solutions to equation (2.2) on the surface of a sphere and discuss their relevance for calcium fertilisation waves.

3. Nonclassical reduction of the nonlinear reaction diffusion equation

As described above, the classical and nonclassical symmetries of equations of type (1.1) were studied in one dimension (with $u(\mathbf{x},t) = u(x,t)$) by Arrigo & Hill (1995) and in two dimensions (with $u(\mathbf{x},t) = u(x,y,t)$) by Goard & Broadbridge (1996). In both one and two Cartesian dimensions, there is a nonclassical symmetry generator that allows equation (1.1) to be reduced to a linear second order differential equation with one fewer independent variables, provided

$$R(u) = \left(\frac{A}{D(u)} + \kappa\right)\int_{u^*}^{u} D(u')\,\mathrm{d}u'. \tag{3.1}$$

This reduction method does not assume restrictions on the choice of coordinates or the number of dimensions (Broadbridge & Bradshaw-Hajek, 2016; Broadbridge *et al.*, 2015). As demonstrated here, it is still valid when the spatial domain is the surface of an embedded sphere, with the transport process described in terms of the surface Laplacian. The transformation can be defined by the nonclassical symmetry generator,

$$\Gamma = \frac{\partial}{\partial t} + Au\frac{\partial}{\partial u}.$$

We define a new function $\Psi(\theta,\phi)$ that is related to the calcium concentration $u(\theta,\phi,t)$ via

$$\mu = \int_{u^*}^{u} D(u')\,\mathrm{d}u' = \mathrm{e}^{At}\Psi(\mathbf{x}). \tag{3.2}$$

The quantity μ is the flux potential, since the flux density of calcium ions is $-\nabla\mu = -D(u)\nabla u$. The constants A and κ arise from the nonclassical symmetry analysis, while u^* must be appropriately chosen and will be discussed in further detail later.

Equation (3.2) implies that $D(u)\nabla u = \mathrm{e}^{At}\nabla\Psi$. Using this, and assuming that relationship (3.1) is satisfied, equation (1.1) in spherical coordinates may be reduced to

$$\nabla^2\Psi(\mathbf{x}) + \kappa\Psi(\mathbf{x}) = 0, \tag{3.3}$$

i.e. the Helmholtz ($\kappa > 0$), modified Helmholtz ($\kappa < 0$) or Laplace equation ($\kappa = 0$). Here, ∇^2 is the Laplacian on the surface of a sphere, and $\Psi(\mathbf{x}) = \Psi(\theta,\phi)$, where $0 \le \theta \le \pi$ is the polar angle and $0 \le \phi \le 2\pi$ is the azimuthal angle.

Solution of equation (3.3) on the surface of a sphere depends on the value of the parameter κ, but in general it can be written in terms of trigonometric, hypergeometric and associated Legendre functions.

4. Model diffusivity and solution

Nondimensionalisation of the equation in Section 2 has scaled the problem so that $u = 1$ represents the positive stable equilibrium value. Then u_1 is the critical stimulus level, an unstable equilibrium value above which more calcium will be released; $u = 1$ denotes 100% saturation. Equation (2.2) may be reduced to (3.3) whenever the diffusion coefficient and the reaction term satisfy relationship (3.1). That is, we must have

$$D(u) = \frac{A\int_{u^*}^{u} D(u')\mathrm{d}u'}{su(1-u)(u-u_1) - \kappa\int_{u^*}^{u} D(u')\mathrm{d}u'}. \tag{4.1}$$

In order that $D(u)$ does not change sign at an achievable concentration, u^* must either be formally set to be negative or it must be one of the zeros of $R(u)$. If $u^* < 0$,

$$D(u) = \frac{A[C + \int_0^u D(u')\mathrm{d}u']}{su(1-u)(u-u_1) - \kappa\left[C + \int_0^u D(u')\mathrm{d}u'\right]},$$

with $C > 0$. It then immediately follows that

$$D(0) = D(1) = D(u_1) = -A/\kappa. \tag{4.2}$$

Now consider $u^* = 1$. From (4.1) it still follows that

$$D(0) = D(u_1) = -A/\kappa.$$

By making use of a Taylor series expansion near $u = u^* = 1$ and ignoring the terms of order $O((u-u^*)^2)$, we see that

$$\begin{aligned} D(u^*) = D(1) &= \lim_{u\to 1} \frac{A\int_1^u D(u')\mathrm{d}u'}{su(1-u)(u-u_1) - \kappa\int_{u^*}^{u} D(u')\mathrm{d}u'} \\ &= \lim_{u\to 1} \frac{AD(1)(u-1)}{-s(u-1)(1-u_1) - \kappa D(1)(u-1)}, \end{aligned} \tag{4.3}$$

from which it follows that

$$D(u^*) = D(1) = \frac{-A - s(1-u_1)}{\kappa}. \tag{4.4}$$

From the above discussion, we see that the constants A and κ must be chosen such that $-A/\kappa > 0$, so that one of these constants must be negative, and one positive. We choose $A < 0$ (and $\kappa > 0$) otherwise the experimentally observed steady state would not be attained.

Relationship (3.1) gives a direct construction of $R(u)$ from a specified diffusivity function $D(u)$; however, we wish to specify $R(u)$ (not $D(u)$). After specifying a cubic reaction function, equation (4.1) cannot be solved exactly to construct $D(u)$ in terms of familiar functions. Numerical solution is relatively

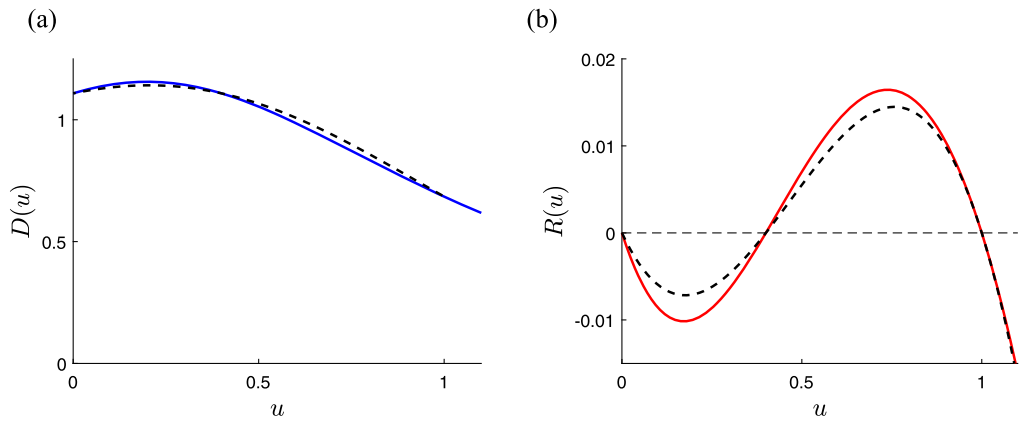

FIG. 1. (a) Nondimensional nonlinear diffusion calculated using the first iterate of the contraction map (4.5), i.e. (4.7) (solid blue line) and the numerical solution of (4.1) (dashed black line). (b) Nondimensional nonlinear reaction term. The black dashed line is a cubic ($su(1-u)(u-u_1)$), and the red solid line is the reaction term that corresponds to (4.7) through (3.1). The parameter values are given in the text (Colour online).

straight forward. Alternatively, a contraction map may be derived that has the solution of (3.1) as its fixed point (Broadbridge *et al.*, 2015),

$$D_{n+1}(u) = \frac{A\int_{u^*}^{u} D_n(u')\mathrm{d}u'}{R(u) - \kappa\int_{u^*}^{u} D_n(u')\mathrm{d}u'}, \tag{4.5}$$

with $D_0(u) = D(u^*)$, allowing an approximate expression for the required diffusion coefficient to be calculated. Since D_0 is a constant, D_1 may always be found analytically, regardless of the form of $R(u)$. The possibility of calculating the second iterate, D_2, analytically will depend on whether or not the integral of D_1 can be found analytically. Fortunately, this map converges quickly and it is often sufficient to use the first iterate (see Fig. 1(a) for a comparison between the numerical solution of equation (4.1) and the first iterate). Although $D(u)$ will be nonconstant and may be non-monotonic, it is not strongly varying, so that solutions $u(\theta, \phi, t)$ are expected to be qualitatively similar to those obtained from a constant diffusivity $D = -A/\kappa$. In fact we will see that the required nonlinear diffusivity decreases with concentration near the saturation level. Wagner & Keizer (1994) proposed a theoretical model for the diffusion coefficient of buffered calcium ions in cytosol and compared their theoretical predictions with the experimental results of Allbritton *et al.* (1992), where the diffusion of calcium ions in cytosol was investigated. The theoretical model of Wagner & Keizer predicts that the diffusion coefficient should increase with increasing calcium ion concentration. The nonlinear diffusion used here is not in alignment with this; however, given that it is not strongly varying, we expect that the predicted calcium profiles will be similar to those obtained using constant diffusion (in fact, the profiles obtained using an increasing diffusion coefficient are also similar (see Wagner & Keizer)). Indeed, the numerical comparison presented in Section 5 supports this claim.

Taking this approach we begin with a cubic reaction term (2.2) and use the contraction map (4.5) to calculate an approximate corresponding nonlinear diffusion. To ensure that we find an exact analytic solution, we then calculate a new reaction term which corresponds exactly to the nonlinear diffusion by using equation (3.1). We show that this new reaction term maintains all the important features of the original cubic reaction term.

In some experiments, fertilisation initiates a wave of calcium ions at one point on the surface of the egg (denoted the animal pole) which is seen to move around the surface of the egg to the opposite pole (the vegetal pole)(Carroll *et al.*, 2003). In this case, there is symmetry in the azimuthal angle (ϕ) and equation (3.3) can be simplified to

$$\frac{1}{\sin\theta}\frac{\mathrm{d}}{\mathrm{d}\theta}\left[\sin\theta\frac{\mathrm{d}\Psi}{\mathrm{d}\theta}\right]+\kappa\Psi=0, \tag{4.6}$$

where $\Psi = \Psi(\theta)$. We choose the starting point of the iterative contraction map for $D(u)$ to be the constant $D_0 = D(1)$ given in (4.4) and the first iterate of the contraction map is given by

$$D_1(u)=\frac{AD_0}{-su(u-u_1)-\kappa D_0}. \tag{4.7}$$

We will use this form of nonlinear diffusion. The nonlinear reaction term that is precisely related to (4.7) by equation (3.1), and thereby allows use of the nonclassical symmetry, can be easily calculated and is shown in Fig. 1. The reaction term is no longer a cubic function; however, it retains many of the features of the cubic that was used to calculate $D(u)$.

Equation (4.6) can be transformed into the Legendre equation via $z = \cos\theta$ (Polyanin & Zaitsev, 2003), and solutions can be written in terms of the hypergeometric function (Abramowitz & Stegun, 1964),

$$\Psi(\theta)=c_1F\left(-\tfrac{\ell}{2},\tfrac{1+\ell}{2};\tfrac{1}{2};\cos\theta\right)+c_2\cos\theta F\left(\tfrac{1-\ell}{2},1+\tfrac{\ell}{2};\tfrac{3}{2};\cos\theta\right),$$

where $\kappa = \ell(\ell+1)$ and c_1, c_2 are constants of integration. The hypergeometric function is a generalisation of the Legendre function that allows the integer index of a Legendre function to extend to non-integer real numbers ℓ. Here we choose $\ell < 1$ (see below for more detail) and so the hypergeometric function is used. In order to ensure that the solution $u(\theta, t)$ initially has little mass in the region away from the animal pole, we choose $c_2 = 0$. The solution for the calcium ion concentration can be found by inverting (3.2) to find

$$u(\theta,t)=\frac{u_1}{2}+b\tan\left(\mathrm{e}^{At}\Psi(\theta)+\tan^{-1}\left(\frac{1-u_1/2}{b}\right)\right), \tag{4.8}$$

where

$$b=\sqrt{\tfrac{\kappa D_0}{s}-\tfrac{1}{4}u_1^2}\,.$$

Solution (4.8) is an exact analytic solution to equation (1.1) with $D(u)$ given by (4.7) and $R(u)$ given by (3.1) in the case of azimuthal symmetry. The constant c_1 may be chosen by requiring that the calcium ion concentration at the bottom (vegetal pole) of the egg is initially zero, that is $u(\pi, 0) = 0$. For $\ell < 1$, the hypergeometric function is unbounded when the argument is 1, i.e. at the site of fertilisation (the animal pole), $\theta = 0$ (see below for an explanation of why we have chosen $\ell < 1$). This localised problem may be resolved by restricting the domain to the exterior of a small 'polar cap' approximating a puncture,

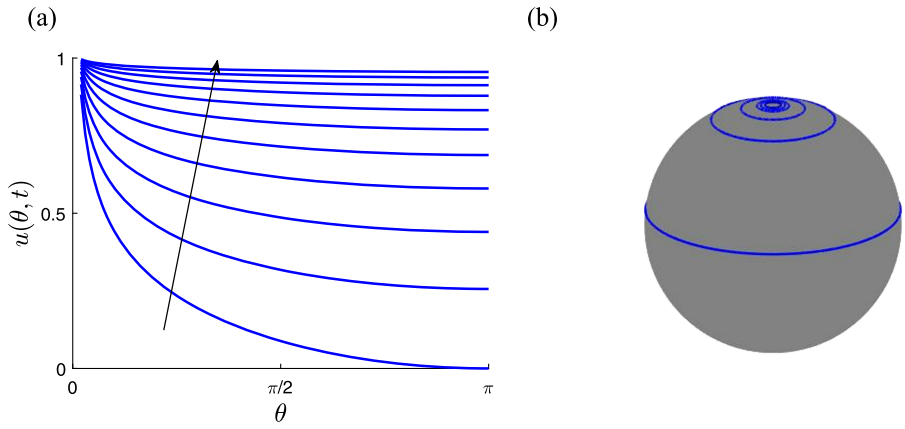

FIG. 2. (a) The nondimensional calcium ion concentration (4.8), the arrow shows increasing time ($t = 0, 1, 2, \ldots, 10$). (b) Progression of calcium ion front on the surface of a sphere. Curves are plotted where $u = 0.85$ at $t = 0, 1, 2, \ldots, 6$. The parameter values are given in the text.

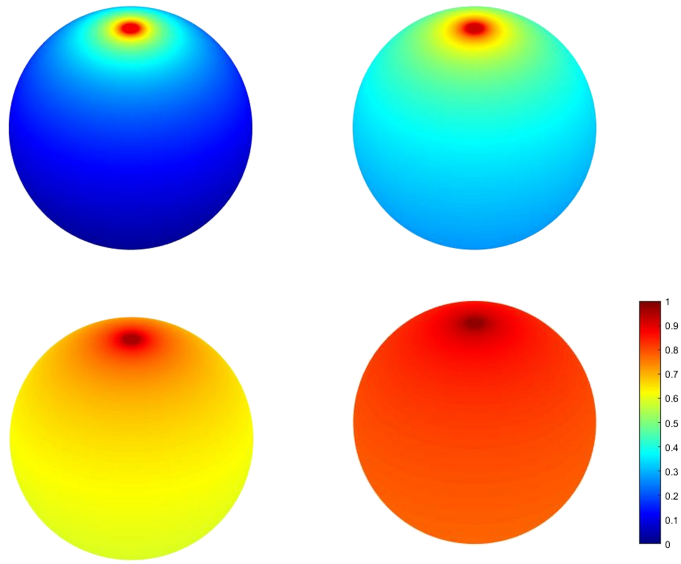

FIG. 3. Nondimensional calcium ion concentration (4.8) mapped onto a sphere for $t = 0,\ 1,\ 3,\ 5$. The parameter values are given in the text.

i.e. $\theta_0 \leq \theta \leq \pi$ (with a small θ_0 representing the size of the puncture). This small polar cap acts a source of calcium ions.

The diffusion and reaction terms are plotted in Fig. 1 and the calcium ion concentration (solution (4.8)) is plotted in Fig. 2. The time evolution of the solution is mapped onto the surface of a sphere in Fig. 3.

In Figs. 1–3, the parameters have been chosen to reflect the dynamics of a calcium wave on the surface of a sea urchin egg such as that observed in the paper by Carroll *et al.* (2003). Sea urchin eggs are approximately 170μm in diameter, so we take $a = 85\mu$m. The parameter A governs the time a calcium wave takes to travel from the top of the egg (the fertilisation site) to the bottom in our model. Experiments show that for a sea urchin egg, this is approximately $\bar{\tau} = 45s$. We choose $\bar{A}$ so that this represents the time taken until the calcium ion concentration is 80% of saturation, $\bar{A} = \ln 0.2/\bar{\tau} \approx -0.035$. While the maximum and minimum calcium concentrations are not given in the paper by Carroll *et al.* (2003) , others suggest $\bar{u}_{\min} = 0\mu$M, $\bar{u}_{\max} = 1\mu$M and $\bar{u}_1 \approx 0.4\mu$M (Slepchenko *et al.*, 2000).

Since we have not taken specific account of the resequestration of the calcium ions, we use the diffusion coefficient for calcium ions in cytoplasm. Various values appear in the literature. A value of $4 \times 10^{-11}\text{m}^2\text{s}^{-1}$ has been used in several papers modelling calcium fertilisation waves (Bugrim *et al.*, 2003; Dupont & Dumollard, 2004). Cheer *et al.* (1987) states that the diffusion coefficient of calcium ions in cytoplasm is approximately $10^{-12}\text{m}^2\text{s}^{-1}$. The diffusion coefficient in the cytoplasm of a nerve axon has been measured as $2 - 5 \times 10^{-10}\text{m}^2\text{s}^{-1}$ (Al-Baldawi & Abercrombie, 1995; Donahue & Abercrombie, 1987), while Allbritton *et al.* (1992) measured it to be $2 \times 10^{-10}\text{m}^2\text{s}^{-1}$ in cytosolic extract from a *Xenopus* oocyte. Here, we take a value of $D(1) = D_0 = 5 \times 10^{-10}\text{m}^2\text{s}^{-1}$.

An appropriate value for the reaction constant s does not seem to appear in the literature. Nevertheless, our methodology allows us to find a relationship between the various parameters so that $\bar{s}$ may be found from the dimensional version of equation (4.4).

The value chosen for κ will determine the shape of the hypergeometric function that is used to construct the solution for the calcium ion concentration. Since $D(u) > 0$ for $0 \leq u \leq 1$, the Kirchhoff variable (calculated using $u^* = 1$) is negative, i.e. $\mu(u) \leq 0$ for $0 \leq u \leq 1$ (see equation (3.2)). It is therefore essential that $\Psi(\theta)$ is negative for $\theta_0 < \theta < \pi$, and as a result the hypergeometric function must not change sign in this range. This only occurs for small values of ℓ, and certainly $\ell < 1$. Here we have chosen $\ell = 0.25$ so that $\kappa = 0.3125$.

Figure 1 shows the nondimensional nonlinear diffusivity calculated using the first iterate of the contraction map (4.5). The nonlinear diffusion is well behaved and near 1 in the range of calcium ion concentrations of interest. The nondimensional nonlinear reaction term calculated using (3.1) is shown in Fig. 1, and it is clear that over the range of concentrations of interest, it exhibits many of the same features of the original cubic reaction term (shown with a dashed line).

The time evolution of the calcium ion concentration is shown in Fig. 2(a). If $A < 0$, then by (3.2), $|\mu(u)|$ will be decreasing with time and $\mu(u)$ will approach zero from below. This means that as time progresses, the solution $u(\theta, t)$ will approach 1 everywhere in a pointwise manner. This can be observed in Fig. 2(a). The effect of introducing a polar cap can be seen near $\theta = 0$, where no solution is shown. As required, the initial calcium ion concentration is zero at the bottom of the egg, $u(\pi, 0) = 0$. The calcium ion concentration is approximately 80% of saturation everywhere at nondimensional time, $t = 5$, corresponding to a dimensional time of $\bar{t} = 50$s, very close to the estimated flooding time for a sea urchin egg. Figure 2(b) shows the latitude at which the nondimensional calcium ion concentration is 85% of saturation, $u = 0.85$, at various times. The increase in concentration is much faster in the lower half of the egg due to the stimulated release of calcium ions from the cortex. Figure 3 shows the solution mapped onto the surface of a sphere, with the final panel showing the concentration at $t = 5$. While the analytic solution (4.8) is not of travelling wave form (i.e. it cannot be written in terms of a travelling wave coordinate, $z = x - ct$), the solution as presented in Fig. 3 appears to the observer as a 'wave' of calcium ions moving over the surface of the egg, exhibiting similar characteristics to those observed in experiment (Carroll *et al.*, 2003).

5. An approximate linearised model

In some situations, the calcium ion fertilisation wave appears as a spiral around the surface of the egg (Lechleiter *et al.*, 1991). This type of behaviour has also been observed in chemical reactions (Maselko & Showalter, 1989), and some numerical solutions of the relevant equations show spiral-like properties. In this section, we find an analytic spiral solution to an approximate linear model.

We are now interested in a model that does not exhibit symmetry in the azimuthal angle, so the calcium ion concentration on the surface of a sphere will be governed by equation (2.2) where ∇ is the usual gradient operator on the surface of a sphere, taking into account variations in both the polar and azimuthal angles, with $u(\theta, \phi, t)$.

Solutions to the Helmholtz equation may be written in terms of spherical harmonics, $Y_l^m(\theta, \phi)$. Taking linear combinations of spherical harmonics of neighbouring degrees (i.e. ℓ and $(\ell + 1)$), spiral patterns can be produced, with the number of 'arms' in the spiral determined by ℓ (Sigrist & Matthews, 2011) . In order to use this property, we must construct solutions using different values of ℓ, and hence different values of κ since $\kappa = \ell(\ell + 1)$. Since the parameter κ is a characteristic of the nonclassical symmetry transformation, directly taking two values of κ is not possible. However, an alternative approach may be taken if we linearise the model equation (2.2).

Using two different values of κ, $\kappa^{(1)}$ and $\kappa^{(2)}$, we may use the first iterate of the contraction map (4.5) to calculate two different nonlinear diffusion functions, $D^{(1)}(u)$ and $D^{(2)}(u)$, that approximately correspond (via (3.1)) to a cubic reaction term. These two functions, may then be used to calculate two different reaction terms, $R^{(1)}(u)$ and $R^{(2)}(u)$, that correspond precisely to the two different nonlinear diffusion terms. We now have two (albeit very similar) model equations

$$u_t = \nabla.(D^{(1)}(u)\nabla u) + R^{(1)}(u) \tag{5.1}$$

$$u_t = \nabla.(D^{(2)}(u)\nabla u) + R^{(2)}(u). \tag{5.2}$$

Note that if we set parameters D_0 and s to be the same in both cases, then choosing different values of κ requires that we also use different values for A (the other parameter arising from the symmetry reduction). These values can be calculated by rearranging (4.4) (with $D_0 = D(1)$). As will be shown, both $R^{(1)}(u)$ and $R^{(2)}(u)$ are very similar to a cubic reaction term.

As the calcium ion concentration approaches its stable equilibrium value, $u = 1$ (Kazmierczak *et al.*, 2018), equation (2.2) may be linearised. The reaction term approximates a linear function, and the nonlinear diffusion may be taken as constant so that both equation (5.1) and equation (5.2) can be approximated by

$$u_t \approx D\nabla^2 u + s(1 - u)(1 - u_1). \tag{5.3}$$

Equation (5.3) is also a linear approximation of equation (2.2).

The nonclassical symmetry described in Section 3 can be used to reduce equations (5.1) and (5.2) to the Helmholtz equation, each with a different parameter,

$$\nabla^2\Psi^{(1)} + \kappa^{(1)}\Psi^{(1)} = 0 \tag{5.4}$$

$$\nabla^2\Psi^{(2)} + \kappa^{(2)}\Psi^{(2)} = 0. \tag{5.5}$$

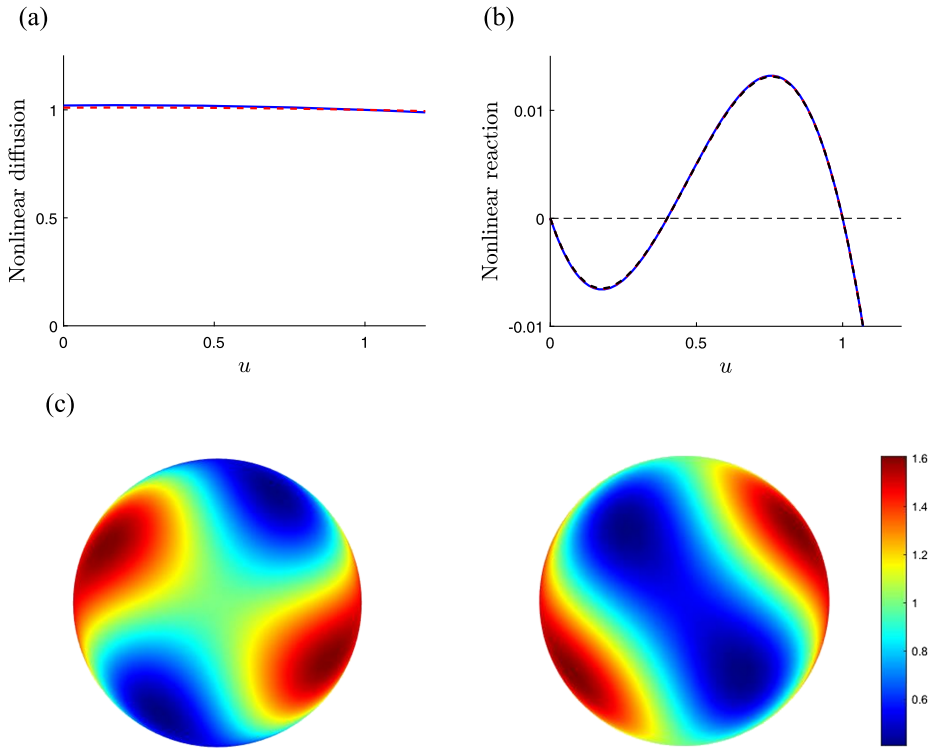

FIG. 4. (a) Nonlinear diffusion coefficient calculated from the first iterate of the contraction map (4.5) with $R(u)$ cubic. The solid (blue) line is calculated with $\kappa^{(1)} = 6$, while the dashed (red) line is for $\kappa^{(2)} = 12$. (b) Nonlinear reaction terms calculated using equation (3.1). The solid (blue) line is calculated with $\kappa^{(1)}$, while the dashed (red) line is for $\kappa^{(2)}$. The finer dashed (black) line is a cubic. The three lines are almost indistinguishable. (c) A top and side view of the calcium ion concentration on the surface of a sphere. The parameter values are $D_0 = 1$, $u_1 = 0.4$ and $s = 0.2$ (Colour online).

The solution to each of these equations can be written in terms of spherical harmonics. By choosing $\kappa^{(1)} = \ell^{(1)}(\ell^{(1)} + 1)$ and $\kappa^{(2)} = \ell^{(2)}(\ell^{(2)} + 1)$ such that $\ell^{(2)} = \ell^{(1)} + 1$, we may take advantage of the fact that neighbouring spherical harmonics can produce spiral patterns on the surface of a sphere.

For example, if we choose $\kappa^{(1)} = 6$ so that $\ell^{(1)} = 2$ and $\kappa^{(2)} = 12$ so that $\ell^{(2)} = 3$, solutions to equations (5.4) and (5.5) may be written

$$\Psi^{(1)}(\theta,\phi) = c_1 Y_2^2(\theta,\phi) = \tfrac{1}{6}\cos 2\phi \sin^2\theta \quad \text{and}$$
$$\Psi^{(2)}(\theta,\phi) = c_2 Y_3^2(\theta,\phi) = \tfrac{1}{3}\sin 2\phi \cos\theta \sin^2\theta.$$

Solutions to equations (5.1) and (5.2) can then be constructed using an appropriate version of (4.8) (where the appropriate values of κ and A are used). These solutions are both approximate solutions to

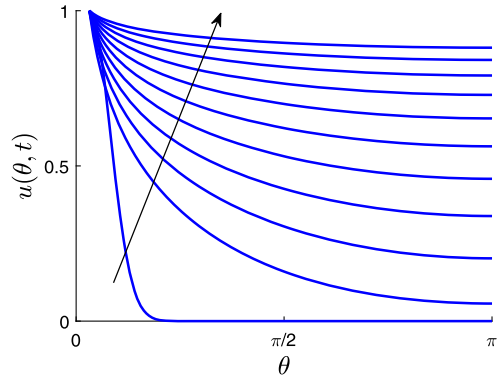

FIG. 5. Numerical solution to equation (2.2) with $D(u) = D$ (constant). The arrow shows increasing time ($t = 0, 1, 2, \ldots, 10$). The parameter values are given in the text.

equation (5.3), and since (5.3) is linear, we may take a linear combination of them. Since (5.3) also approximates (2.2), we find that an example approximate solution to (2.2) is

$$u(\theta,\phi,t) = \tfrac{1}{2}\left[\tfrac{u_1}{2} + b^{(1)}\tan\left(\mathrm{e}^{A^{(1)}t}\Psi^{(1)} + \tan^{-1}\left(\tfrac{1-u_1/2}{b^{(1)}}\right)\right)\right] + \tfrac{1}{2}\left[\tfrac{u_1}{2} + b^{(2)}\tan\left(\mathrm{e}^{A^{(2)}t}\Psi^{(2)} + \tan^{-1}\left(\tfrac{1-u_1/2}{b^{(2)}}\right)\right)\right],$$

where $b^{(1)}$ and $b^{(2)}$ take the same form as b defined earlier.

This solution is shown in Fig. 4, together with the corresponding nonlinear diffusion and nonlinear reaction terms. Figure 4(a) shows that the nonlinear diffusion terms formed using different values for κ are indeed near constant and very similar to each other. The calculated reaction terms, shown in Fig. 4(b), are also very similar, and indeed they are almost cubic in the domain of interest. The solution (Fig. 4(c)) shows a spiral pattern of calcium ions on the surface of the sphere. The spiral has two arms of high calcium ion concentration since we have chosen $\ell^{(1)} = 2$. The spiral pattern is transient since the higher level spherical harmonics decay faster than the lower ones and eventually the interplay between the neighbouring harmonics is lost. As time becomes large, the (nondimensional) calcium ion concentration approaches $u = 1$ everywhere.

6. Discussion and final remarks

In this paper, we have presented the first exact analytic solution to a nonlinear reaction-diffusion equation that describes the calcium ion fertilisation wave on the surface of an egg in the case where the wave moves symmetrically from the sperm entry point to the opposite pole of the egg. This analytic solution reflects the behaviour observed in experiments and is reminiscent of a 'wave' of ions moving over the surface of the egg.

The exact analytic solution presented here may also be compared to the numerical solution of equation (2.2) on the surface of a sphere, shown in Fig. 5. Here, we have set $D(u) = D =$constant so that a comparison with the typical case of constant diffusivity may be made. All nondimensional parameters have been chosen to have the same value as those used to create Fig. 2, with $D = 1$ since this is the average value of the nondimensional nonlinear diffusion. The initial condition (Gaussian)

has been chosen to represent an initial, localised increase in the calcium ion concentration due to a fertilisation event, while the boundary condition at the edge of the polar cap has been set to $u(\theta_0, t) = 1$. The boundary condition at the bottom pole is $u_\theta|_{\theta=\pi} = 0$ for symmetry. Concentrations are shown at the same nondimensional times as those shown in Fig. 2. The numerical solution is very similar to the analytical solution, except at the initial condition and at very early times ($t < 1$). It also exhibits a slight delay in comparison to the analytic solution. This may represent the time taken for the concentration profile in the analytic solution to increase from the 'true' near-zero initial condition to our first contour.

One benefit of obtaining an analytical solution is that it enables various features to be investigated that might be elusive given a numerical solution only. For example, even though the solution presented here (4.8) is infinite at the top (animal pole) of the egg (as discussed in Section 4), the derivative is not, so that the flux of calcium ions from the fertilisation site may be directly calculated. In this way, we may gain an understanding of what proportion of calcium ions originates from the fertilisation site, and what proportion is released from the cortex of the egg. The analytic model has a boundary condition of flux density being proportional to $\mathrm{e}^{-|A|t}$. The solution with constant concentration at the aperture also has rapidly decreasing flux density. The numerical and analytical solutions become comparable after a short time.

The nondimensional flux from the vicinity of the animal pole is given by

$$\begin{aligned} 2\pi \left| \lim_{\theta\to 0}(-\sin\theta \nabla\mu) \right| &= -2\pi \mathrm{e}^{At} \lim_{\theta\to 0} \sin\theta \frac{\mathrm{d}}{\mathrm{d}\theta}\Psi(\theta) \\ &= 2c_1\pi^{3/2}\mathrm{e}^{At}\left[\Gamma\left(-\tfrac{\ell}{2}\right)\Gamma\left(\tfrac{1+\ell}{2}\right)\right]^{-1}. \end{aligned}$$

The total amount of calcium ions released from the animal pole can be found by integrating the flux from the time when the calcium concentration at the vegetal pole is zero,

$$2c_1\pi^{3/2}\left[\Gamma\left(-\tfrac{\ell}{2}\right)\Gamma\left(\tfrac{1+\ell}{2}\right)\right]^{-1}\int_0^\infty \mathrm{e}^{At'}\mathrm{d}t = \frac{-2c_1\pi^{3/2}}{A\Gamma\left(-\tfrac{\ell}{2}\right)\Gamma\left(\tfrac{1+\ell}{2}\right)} \tag{6.1}$$

since $A < 0$.

The total nondimensional amount of calcium ions that has been released over the surface of the egg both from the animal pole and from the stored reserves near the cortex can be found by calculating the surface integral of concentration deficiency over the sphere,

$$2\pi\int_0^\pi (1 - u(\theta', 0))\sin\theta'\mathrm{d}\theta', \tag{6.2}$$

since $u = 1$ represents nondimensional calcium ion saturation. Unfortunately, this quantity cannot be calculated analytically; however, a numerical calculation is straightforward.

Given these two quantities, (6.1) and (6.2), the amount of calcium ions released from the cortex can be obtained by calculating the difference. Using the parameter values given in Section 4, we find that approximately 81% of the calcium ions are released from the cortex of the egg, while 19% of the total increase in calcium ions comes from the flux from the pole. The cortical store of calcium is important in this role, with the calcium ions flowing from the pole serving mainly as a trigger for cortical activity. The diffusive time scale is much larger than the characteristic time for the reaction dynamics ($T_d \gg T_r$), ensuring that the release of calcium ions from the cortex contributes significantly to the dynamics (c.f. (Spiro & Othmer, 1999)).

In this analysis, we have assumed that the calcium wave has progressed as a surface wave on the plasma membrane; in this way we have removed the radial dependence of the problem. However, this is an approximation and it is likely that the waves actually extend some distance into the interior of the egg (Fall *et al.*, 2004). The concentrations that we predict here could be viewed as an average over a small radial distance near the surface of the egg. Alternatively, the particular nonclassical symmetry used to reduce equation (2.2) to the Helmholtz equation (3.3) can also be used to construct solutions in the case when the behaviour of the calcium ion concentration inside the egg becomes important. We leave this for a future investigation.

References

Abramowitz, M. & Stegun, I. A. (1964) *Handbook of Mathematical Functions with Formulas, Graphs, and Mathematical Tables* Applied Mathematics Series 55. Washington, DC: National Bureau of Standards.

Al-Baldawi, N. F. & Abercrombie, R. F. (1995) Calcium diffusion coefficient in Myxicola axoplasm. *Cell Calcium*, **17**, 422–430.

Allbritton, N. L., Meyer, T. & Stryer, L. (1992) Range of messenger action of calcium ion and inositol 1, 4, 5-trisphosphate. *Science*, **258**, 1812–1815.

Arrigo, D. J. & Hill, J. M. (1995) Nonclassical symmetries for nonlinear diffusion and absorption. *Stud. Appl. Math.*, **94**, 21–39.

Arrigo, D. J., Hill, J. M. & Broadbridge, P. (1994) Nonclassical symmetry reductions of the linear diffusion equation with a nonlinear source. *IMA J. Appl. Math.*, **52**, 1–24.

Broadbridge, P. & Bradshaw-Hajek, B. H. (2016) Exact solutions for logistic reaction-diffusion equations in biology. *Z. Angew. Math. Phys.*, **67**, 93.

Broadbridge, P., Bradshaw-Hajek, B. H. & Triadis, D. (2015) Exact nonclassical symmetry solutions of Arrhenius reaction-diffusion. *Proc. A.*, **471**, 20150580.

Bugrim, A., Fontanilla, R., Eutenier, B.B., Keizer, J. & Nuccitelli, R. (2003) Sperm initiate a Ca^{++} wave in frog eggs that is more similar to Ca^{++} waves initiated by IP_3 than by Ca^{++}. *Biophys. J.,* **84**, 1580–1590.

Carroll, M., Levasseur, M., Wood, C., Whitaker, M., Jones, K. T. & McDougall, A. (2003) Exploring the mechanism of action of the sperm-triggered calcium-wave pacemaker in ascidian zygotes. *J. Cell Sci.*, **116**, 4997–5004.

Cheer, A., Vincent, J.-P., Nuccitelli, R. & Oster, G. (1987) Cortical activity in vertebrate eggs. I: The activation waves. *J. Theor. Biol.*, **124**, 377–404.

Chen, D. Y. & Gu, Y. (1999) Cole–Hopf quotient and exact solutions of the generalised Fitzhugh–Nagumo equations. *Acta Math. Sci. (Chinese)*, **19**, 7–14.

Chen, Z. X. & Guo, B. Y. (1992) Analytic solutions of the Nagumo equation. *IMA J. Appl. Math.*, **48**, 107–115.

Clarkson, P. A. & Mansfield, E. L. (1994) Symmetry reductions and exact solutions of a class of nonlinear heat equations. *Phys. D*, **70**, 250–288.

Conte, R. (1988) Universal invariance properties of Painlevé analysis and Bäcklund transformation in nonlinear partial differential equations. *Phys. Lett. A*, **134**, 100–104.

Cuthbertson, K. R., Whittingham, D. G. & Cobbold, P. H. (1981) Free Ca^{2+} increases in exponential phases during mouse oocyte activation. *Nature,***294**, 754–757.

Donahue, B. S. & Abercrombie, R. F. (1987) Free diffusion coefficient of ionic calcium in cytoplasm. *Cell Calcium*, **8**, 437–448.

Dupont, G. & Dumollard, R. (2004) Simulation of calcium waves in ascidian eggs: insights into the origin of the pacemaker sites and the possible nature of the sperm factor. *J. Cell Sci.*, **117**, 4313–4323.

Fall, C.P., Wagner, J.M., Loew, L.M. & Nuccitelli, R. (2004) Cortically restricted production of IP_3 leads to propagation of the fertilization Ca^{2+} wave along the cell surface in a model of the *Xenopus egg. J. Theor. Biol.*, **231**, 487–496.

Galaktionov, V. A., Dorodnitsyn, V. A., Elenin, G. G., Kurdyumov, S. P. & Samarskii, A. A. (1988) A quasilinear heat equation with a source: peaking, localization, symmetry exact solutions, asymptotics, structures. *J. Sov. Math.*, **41**, 1222–1292.

Gilkey, J. C. (1983) Roles of calcium and pH in activation of eggs of the medaka fish, *Oryzias latipes*. *J. Cell Biol.*, **97**, 669–678.

Goard, J. M. & Broadbridge, P. (1996) Nonclassical symmetry analysis of nonlinear reaction-diffusion equations in two spatial dimensions. *Nonlinear Anal.*, **26**, 735–754.

Kametaka, Y. (1976) On the nonlinear diffusion equation of Kolmogorov–Petrovskii–Piskunov type. *Osaka J. Math.*, **13**, 11–66.

Kawahara, T. & Tanaka, M. (1983) Interactions of travelling fronts: an exact solution of a nonlinear diffusion equation. *Phys. Lett. A*, **97**, 311–314.

Kazmierczak, B., Tsai, J. C. & Slawomir, B. (2018) The propagation phenomenon of solutions of a parabolic problem on the sphere. *Math. Models Methods Appl. Sci.*, **28**, 2001–2067.

King, J. R. (1990) Exact similarity solutions to some nonlinear diffusion equations. *J. Phys. A: Math. Gen.*, **23**, 3681–3697.

Lane, D. C., Murray, J. D. & Manoranjan, V. S. (1987) Analysis of wave phenomena in a morphogenetic mechanochemical model and an application to post-fertilization waves on eggs. *Math. Med. Biol.*, **4**, 309–331.

Lechleiter, J., Girard, S., Peralta, E. & Clapham, D. (1991) Spiral calcium wave propagation and annihilation in Xenopus laevis oocytes. *Science*, **252**, 123–126.

Maselko, J. & Showalter, K. (1989) Chemical waves on spherical surfaces. *Nature*, **339**, 609.

McKean, H. P. (1970) Nagumo's equation. *Adv. Math.*, **4**, 209–223.

Murray, J. D. (2002) *Mathematical Biology I. An Introduction.* Interdisciplinary Applied Mathematics, vol. 17. Berlin: Springer.

Nikitin, A. G. & Barannyk, T. A. (2004) Solitary wave and other solutions for nonlinear heat equations. *Cen. Euro. J. Math.*, **2**, 840–858.

Nuccitelli, R. (1991) How do Sperm Activate Eggs? *Curr. Top. Dev. Biol.*, **25**, 1–16.

Polyanin, A. D. & Zaitsev, V. F. (2003) *Handbook of Exact Solutions for Ordinary Differential Equations*. Boca Raton, Florida: Chapman & Hall/CRC.

Ridgway, E. B., Gilkey, J. C. & Jaffe, L. F. (1977) Free calcium increases explosively in activating medaka eggs. *Cell Biol.*, **74**, 623–627.

Sigrist, R. & Matthews, P. (2011) Symmetric spiral patterns on spheres. *SIAM J. Appl. Dyn. Sys.*, **10**, 1177–1121.

Slepchenko, B. M., Schaff, J. C. & Choi, Y. S. (2000) Numerical approach to fast reactions in reaction-diffusion systems: application to buffered calcium waves in bistable models. *J. Comput. Phys.*, **162**, 186–218.

Sneyd, J., Dale, P. D. & Duffy, A. (1998) Traveling waves in buffered systems: applications to calcium waves. *SIAM J. Appl. Math.*, **58**, 1178–1192.

Sneyd, J., Girard, S. & Clapham, D. (1993) Calcium wave propagation by calcium-induced calcium release: an unusual excitable system. *Bull. Math. Biol.*, **55**, 315–344.

Spiro, P. A. & Othmer, H. G. (1999) The effect of heterogeneously-distributed RyR channels on calcium dynamics in cardiac myocytes. *Bull. Math. Biol.*, **61**, 651–681.

Steinhardt, R., Zucker, R. & Schattenand, G. (1977) Intracellular calcium release at fertilisation in the sea urchin egg. *Dev. Biol.*, **58**, 185–196.

Tsai, J.-C. & Sneyd, J. (2007) Are buffers boring? Uniqueness and asymptotical stability of traveling wave fronts in the buffered bistable system. *J. Math. Biol.*, **54**, 513–553.

Wagner, J., Lie, Y-X., Pearson, J. & Keizer, J. (1998) Simulation of the fertilization Ca^{2+} wave in *Xenopus laevis eggs. Biophys. J.*, **75**, 2088–2097.

Wagner, J. & Keizer, J. (1994) Effects of rapid buffers on Ca^{2+} diffusion and Ca^{2+} oscillations. *Biophys. J.*, **67**, 447–456.

Wasserman, W. J., Pinto, L. H., O'Connor, C. M. & Smith, L. D. (1980) Progesterone induces a rapid increase in $[Ca^{2+}]_{in}$ of Xenopus laevis oocytes. *Proc. Natl. Acad. Sci. U. S. A.*, **77**, 1534–1536.